Table look-up variable structure control for robotic arms

Ying J. Huang and **Shin H. Chang**

Department of Electrical Engineering
Yuan Ze University
135 Far-East Rd, Chung-Li , Taiwan, ROC
E-mail: eeyjh@saturn.yzu.edu.tw

Abstract

In this paper, a variable structure control method with look-up table is proposed and applied to nonlinear time-varying manipulator. The robustness in control system against parametric variations and external disturbance is achieved. Suitable part of control torque is picked up from the established angle-related table. The primary purpose of this design is to lower the level of calculation complexity so that calculation time can be greatly decreased in actual machine robot arm application. Another important advantage is that joint angular velocities are not necessary to measure or observe.

Keywords-variable structure control; sliding mode; robustness; robotics; look-up table

1 Introduction

Variable structure control (VSC) has been developed by many mathematicians and engineers [1, 2, 3, 4]. Fundamentally, VSC consists of two or more sub-systems. Depending on switching control law, the system trajectory is forced to move toward the pre-defined sliding hypersurfaces. The system trajectory will stay and move toward the designed control target on the intersection of sliding hypersurfaces asymptotically as soon as the system trajectory enters the sliding mode.

Robots have been applied widely in industry field for decades. A large range of application has been found [5, 6, 7, 8]. Many researchers have developed various control methods for nonlinear robot manipulators to achieve different tasks [9, 10, 11, 12]. There are usually complicated mathematical formulas to be calculated in the control law. Inevitably, it needs expensive prime cost and consumes a lot of computing time.

In this paper, according to motion variation of robot manipulator for each joint angle, several sections of motion can be distinguished and look-up tables can be established. The controller still retains benefits of VSC against parametric variations and external disturbance, or some uncertainties. The advantage of the proposed table look-up variable structure control (TVSC) is that the controller can suitably pick up the control torque rapidly from the established table at each sampling time. It is ensured that a lot of consumption time and prime cost will greatly be reduced. Therefore, a low cost hardware can be achieved.

2 Methodology

2.1 System description

Consider the dynamic equation of an m-link robotic arm that can be represented as

$$\begin{aligned} \dot{x} &= Ax + B\tau + G + w \\ y &= Cx \end{aligned} \tag{1}$$

where $x \in R^{n\times 1}$ is the state vector, $A \in R^{n\times n}$ is the system coefficient matrix, $B \in R^{n\times m}$ is the input coefficient matrix, $\tau \in R^{m\times 1}$ is the control input torque applied at every manipulator joint, $G \in R^{n\times 1}$ is the gravity term, $w \in R^{n\times 1}$ is the external disturbance, $y \in R^{m\times 1}$ is the system output, $C \in R^{m\times n}$ is the output coefficient matrix. Assume the external disturbance w is bounded and $\max|w|$ can be estimated.

The elements of the state vector, $x = [x_1 \quad x_2 \quad \cdots \quad x_n]^T$, contains every joint angles and angular velocities, i.e., $(x_1, x_2, \cdots, x_m)$ is the set of every joint angles and $(x_{m+1}, x_{m+2}, \cdots, x_n)$ is the set of every joint angular velocities. Since x_{i+i} is the derivative of x_i, therefore, the matrices A and B are

$$A = \begin{bmatrix} 0_{m\times m} & I_{m\times m} \\ A_1 & A_2 \end{bmatrix}_{n\times n}, B = \begin{bmatrix} B_1 \\ B_2 \end{bmatrix}_{n\times m}.$$

Define the desired state $x_d = [x_{1d} \quad x_{2d} \quad \cdots \quad x_{nd}]^T$ where x_{id} is the desired trajectory of state x_i. Let the tracking error of every joint be defined as

$$e = [e_1 \quad e_2 \quad \cdots \quad e_n]^T, \tag{2}$$

$$e_i = x_i - x_{id},\ i = 1, 2, \cdots, n. \tag{3}$$

The goal here is to achieve trajectory control, i.e., $e_i \to 0$.

2.2 Sliding function design

Consider the system dynamics (1). The first step in the TVSC design is to design a switching function. Let switching function be chosen as

$$\begin{aligned} \sigma &= [\sigma_1 \quad \sigma_2 \quad \cdots \quad \sigma_m]^T, \\ &= \alpha e, \end{aligned} \tag{4}$$

where

$$\alpha = \begin{bmatrix} c_1 & 0 & \cdots & 1 & 0 & \cdots & 0 \\ 0 & c_2 & 0 & \cdots & 1 & \cdots & 0 \\ \vdots & \vdots & \ddots & \ddots & \ddots & \ddots & \vdots \\ 0 & 0 & \cdots & c_m & 0 & \cdots & 1 \end{bmatrix}_{m \times n}, \tag{5}$$

$$c_1, c_2, \cdots, c_m > 0. \tag{6}$$

When the control law is suitably chosen, any state x outside the switching surface $\{\sigma_i = 0, i = 1, 2, \ldots, m\}$ is driven to reach the surface in finite time. In other words, system trajectory coming from either side of the surface approaches sequentially $\sigma_i = 0$, and eventually $\sigma = 0$. When system trajectory is on the switching surfaces the sliding mode takes place, and the desired system dynamics follows. In the sliding mode, the tracking error dynamic function can be written as

$$\dot{e}_i + c_i e_i = 0,\ i = 1, 2, \cdots, m. \tag{7}$$

During the sliding mode, system dynamics are solely governed by the parameters that describe the line $\sigma_i = 0$. As long as σ_i sustains zero, it is expected that trajectory of x_i stays on the sliding surface and moves toward x_{id} at exponential rate. There will be no tracking error between x_i and x_{id} eventually. In this way, the overall VSC system is globally asymptotically stable.

2.3 Control law design

Next, with the formulation of sliding function (4) we can derive the suitable control law as follows.

By direct computation, differentiating σ yields

$$\begin{aligned} \dot{\sigma} &= \alpha(\dot{x} - \dot{x}_d), \\ &= \alpha A x + \alpha B \tau + \alpha G + \alpha w - \alpha \dot{x}_d. \end{aligned} \tag{8}$$

Equating (8) to be equivalently zero, the equivalent control input torque is found to be

$$\tau = -(\alpha B)^{-1}(\alpha A x + \alpha G) + (\alpha B)^{-1}(\alpha \dot{x}_d - \alpha w). \tag{9}$$

Let $\tau^* = -(\alpha B)^{-1}(\alpha A x + \alpha G)$ and $\mu^* = (\alpha B)^{-1}$. They are expected values and tabulated in Table 1 and 2, depending on different joint angular conditions. Correspondingly, let $\hat{\tau}$ and $\hat{\mu}$ are the picked-up values from the established Table 1 and 2.

Define the estimation errors, $\tau_e = \hat{\tau} - \tau^*$ and $\mu_e = \hat{\mu} - \mu^*$. The maximum variations of μ_e depend on how many segments, in the pick-up tables, we divide. Less segments require smaller database, but the torque estimation error would be larger. On the other hands, more segments require larger database, but the torque estimation error would be smaller. The designers need to trade off the torque precision and the hardware requirement. Nevertheless,

$$\begin{aligned} (\mu^*)^{-1}(\hat{\mu}) &= (\mu^*)^{-1}(\mu^* + \mu_e), \\ &= I + (\mu^*)^{-1}\mu_e. \end{aligned} \tag{10}$$

Assume that the sum of the absolute values of all the elements of each row of the product $(\mu^*)^{-1}\mu_e$ is less than 1, that is

$$\sum_{j=1}^{m} \left| \left[(\mu^*)^{-1}\mu_e \right]_{ij} \right| < 1,\ i = 1, 2, \cdots, m. \tag{11}$$

Let $\varepsilon_i = 1 - \sum_{j=1}^{m} \left| \left[(\mu^*)^{-1}\mu_e \right]_{ij} \right| > 0$, and $\varepsilon = \inf\{\varepsilon_i\},\ i = 1, 2, \cdots, m$.

Theorem: Consider the dynamic system (1) with the switching surface formulation (4). If the control law is chosen as

$$\tau = \hat{\tau} + \hat{\mu}(\alpha \dot{x}_d - \alpha \hat{w} - \beta\, \mathrm{sgn}\, \sigma). \tag{12}$$

where $\hat{w}$ is the estimated value of w, and for $i = 1, 2, \cdots, m$,

$$\beta > \frac{1}{\varepsilon}\left\{\begin{array}{l}\sup\left|\left[\left(\mu^*\right)^{-1}\left(\tau^* - \hat{\tau}\right)\right]_i\right| + \sup\left|\left[\left(\mu^*\right)^{-1}\left(\hat{\mu} - \mu^*\right)\alpha\dot{x}_d\right]_i\right| + \\ \sup\left|\left[\left(\mu^*\right)^{-1}\left(\mu^*\alpha w - \hat{\mu}\alpha\hat{w}\right)\right]_i\right|\end{array}\right\}, \tag{13}$$

then the switching surfaces will be reached in finite time.

Proof: Substituting (12) into (8), the resulting expression of $\dot{\sigma}$ is

$$\begin{aligned}\dot{\sigma} = &-\left(\mu^*\right)^{-1}\left(\tau^* - \hat{\tau}\right) + \left(\mu^*\right)^{-1}\left(\hat{\mu} - \mu^*\right)\alpha\dot{x}_d \\ &+ \left(\mu^*\right)^{-1}\left(\mu^*\alpha w - \hat{\mu}\alpha\hat{w}\right) - \left(\mu^*\right)^{-1}\hat{\mu}\beta\,\mathrm{sgn}\,\sigma\end{aligned} \tag{14}$$

Then we can rewrite (14) as

$$\begin{aligned}\dot{\sigma}_i &= \left\{\begin{array}{l}-\left(\mu^*\right)^{-1}\left(\tau^* - \hat{\tau}\right) + \left(\mu^*\right)^{-1}\left(\hat{\mu} - \mu^*\right)\alpha\dot{x}_d + \left(\mu^*\right)^{-1}\left(\mu^*\alpha w - \hat{\mu}\alpha\hat{w}\right) \\ -\left(I + \left(\mu^*\right)^{-1}\mu_e\right)\beta\,\mathrm{sgn}\,\sigma\end{array}\right\}_i \\ &= \left[-\left(\mu^*\right)^{-1}\left(\tau^* - \hat{\tau}\right)\right]_i + \left[\left(\mu^*\right)^{-1}\left(\hat{\mu} - \mu^*\right)\alpha\dot{x}_d\right]_i \\ &\quad + \left[\left(\mu^*\right)^{-1}\left(\mu^*\alpha w - \hat{\mu}\alpha\hat{w}\right)\right]_i \\ &\quad - \left(1 + \sum_{j=1}^{m}\left[\left(\mu^*\right)^{-1}\mu_e\right]_{ij}\mathrm{sgn}\,\sigma_j\,\mathrm{sgn}\,\sigma_i\right)\beta\,\mathrm{sgn}\,\sigma_i \\ &= -\lambda\,\mathrm{sgn}\,\sigma_i\ ,\end{aligned} \tag{15}$$

where $\lambda > 0$. Therefore, we can obtain a satisfied sliding condition,

$$\sigma_i\dot{\sigma}_i < -\lambda\ . \tag{16}$$

The control system will be guaranteed to reach the sliding mode and sustain on it.

In this paper, according to the Lyapunov stability criterion, the system trajectory reaches hypersurface and moves toward to the control reaches target asymptotically. Finally $\sigma \cong 0$, $e \cong 0$, and $x_i = x_{id}$. The controller shown in section 2 has high-frequency switching (chattering phenomena) near the sliding surface. Chattering is undesirable in practice because it involves high control activity. Note that in practice, these drastic changes of input can be avoided by introducing a boundary layer with width Φ. Thus we replace $\mathrm{sgn}(\sigma)$ with $sat(\sigma/\Phi)$ in (12), and further reduce the computation complication. Let the control law be

$$\tau = \hat{\tau} + \hat{\mu}\left(\alpha\dot{x}_d - \alpha\hat{w} - \beta sat\left(\sigma/\Phi\right)\right), \tag{17}$$

where

$$sat(\varepsilon) = \begin{cases}\varepsilon & , |\varepsilon| \le 1 \\ \mathrm{sgn}(\varepsilon), & |\varepsilon| > 1\end{cases}\ . \tag{18}$$

A two-link robot manipulator is applied in the following.

3 Application example

Consider a nonlinear time-varying two-link robot arm as shown in Figure 1. The system equation can be written as

$$\dot{x} = Ax + B\tau + G =$$

$$\begin{bmatrix}\dot{x}_1\\ \dot{x}_2\\ \dot{x}_3\\ \dot{x}_4\end{bmatrix} = \begin{bmatrix}0 & 0 & 1 & 0\\ 0 & 0 & 0 & 1\\ 0 & 0 & A_{33} & A_{34}\\ 0 & 0 & A_{43} & A_{44}\end{bmatrix}\begin{bmatrix}x_1\\ x_2\\ x_3\\ x_4\end{bmatrix} + \begin{bmatrix}0 & 0\\ 0 & 0\\ B_{31} & B_{32}\\ B_{41} & B_{42}\end{bmatrix}\begin{bmatrix}\tau_1\\ \tau_2\end{bmatrix} + \begin{bmatrix}0\\ 0\\ G_3\\ G_4\end{bmatrix}. \tag{19}$$

where $\begin{bmatrix}A_{33} & A_{34}\\ A_{43} & A_{44}\end{bmatrix}$, $\begin{bmatrix}B_{31} & B_{32}\\ B_{41} & B_{42}\end{bmatrix}$, and $\begin{bmatrix}G_3\\ G_4\end{bmatrix}$ are described in the Appendix. For simplicity of demonstration, here the external disturbance is supposed not involved.

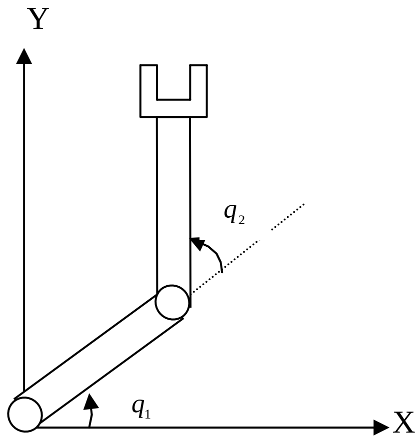

Figure 1: Two-link manipulator

According to (4) and (5), α and σ can be chosen as

$$\alpha = \begin{bmatrix}c_1 & 0 & 1 & 0\\ 0 & c_2 & 0 & 1\end{bmatrix}, \tag{20}$$

$$\sigma = \begin{bmatrix}\sigma_1 & \sigma_2\end{bmatrix}^T = \begin{bmatrix}c_1 e_1 + \dot{e}_1\\ c_2 e_2 + \dot{e}_2\end{bmatrix}. \tag{21}$$

First, assuming $\tilde{\tau}_1$, $\tilde{\tau}_2$, and $\hat{\mu}$ are picked up from the established look-up Table 1 and Table 2. We calculate in advanced the $\tilde{\tau}_1$, $\tilde{\tau}_2$ and $\hat{\mu}$ from -180° to 180° of robot manipulator motion for every interval of 10° wide, and establish the look-up tables. The look-up tables are 37×37 matrices and are shown in Table 1 and Table 2.

In practical implementation, the look-up table will be established according to actual range of operating for actual machine robot arm application. Besides, a character of symmetrical $\tilde{\tau}$ can also be utilized, so that this established table matrix may be constructed less than 37×37 matrix in actual application. To establish less volume of look-up table and to attain precise tracking trajectory are very important. Therefore, the controller picks up rapidly suitable control torque from the established table at every sampling time. A great deal of computation time and expensive cost will be reduced greatly. In the process of establishing, we assume the mean value of the joint angular velocities of two-link in look-up table are

$$\max|\dot{x}_1| = \pi\ ,\ \max|\dot{x}_2| = \pi\ ,$$

$$\text{mean value} = \dot{x}_1 = \dot{x}_2 = \frac{\pi}{2}\ .$$

Because $\tilde{\tau}_1$ and $\tilde{\tau}_2$ are the estimated values at every interval of 10°, the variation of torque remains a torque size at some angles, and changes to different value at other segments. The abruptly change of torque at the boundary is not to be expected.

In order to cancel the abruptly phenomenon, we average the torque at boundary in changing torque. In other word, there is a buffer zone among two differential torques. A new $\hat{\tau}$ in the buffer zone is calculated as

$$\hat{\tau}(K\Delta t) = \frac{1}{2}\left\{\tilde{\tau}(K\Delta t) + \left[\hat{\tau}(K-1)\Delta t\right]\right\}. \qquad (22)$$

The manipulator, initially resting at $q_2 = q_2 = 0$, is driven with a path command of $q_{1d} = 60 + 20\times\cos(\pi t)$ and $q_{2d} = 10 + 40\times\sin(\pi t)$.

According to section 2, we apply the new system control law as

$$\tau = \hat{\tau} + \hat{\mu}\left(\alpha\dot{x}_d - \beta sat(\sigma/\Phi)\right), \qquad (23)$$

where $\hat{\tau}$ is averaged value according to (22) from the established look-up Table 1 and $\hat{\mu}$ is picked up from look-up Table 2. $\beta = 45$. $\Phi = 0.05$. Because of lower the level of calculation complexity in the proposed method, so that it is available the sampling time is chosen as 0.001 seconds in actual system.

The simulation results are shown in Fig. 2 to Fig. 5. The angles of links are shown in Fig. 2. The sliding variables are shown in Fig. 3. The sliding variables need approximately 0.1 seconds to reach the zero. As soon as sliding variables reaches the zero, the tracking error for link 1 will reduce to zero with exponential mode of e^{-3t} rate, and for link 2 with exponential mode of e^{-4t} rate. The tracking error for link 1 needs approximately 1.3 seconds to reach the anticipated angle. The tracking error for link 2 needs approximately 1 seconds to reach the anticipated angle. The torque $\hat{\tau}$ for link 1 is between 2~-23(N), and for link 2 is between -4~-12(N) are shown in Fig. 4. The angular errors are shown in Fig. 5.

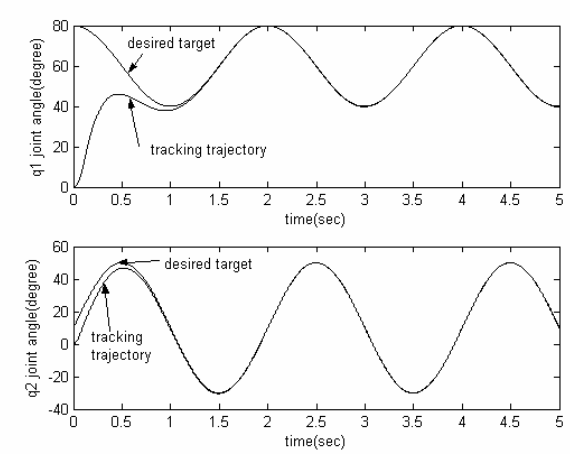

Figure 2: The joint angles q_1 and q_2

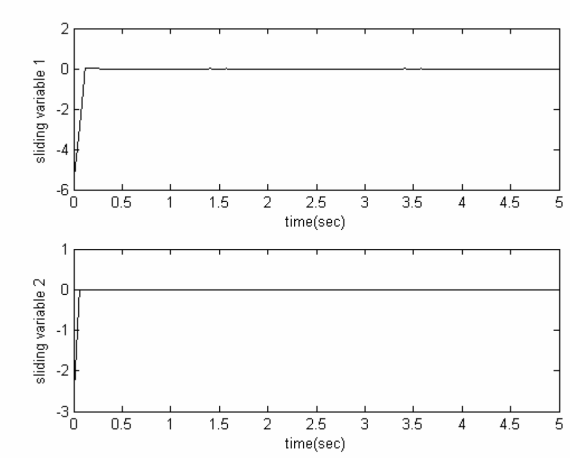

Figure 3: Sliding variables

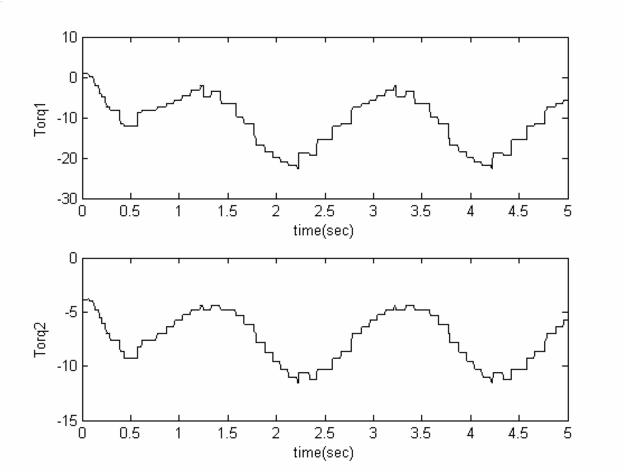

Figure 4: The value of $\hat{\tau}$

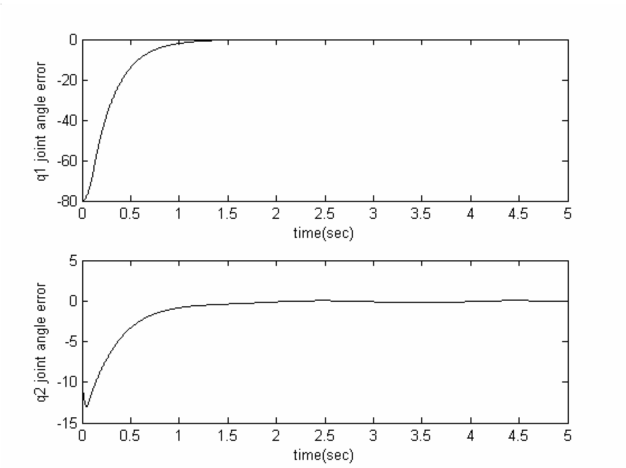

Figure 5: The angular errors

According to simulation results, the advantage of the proposed look-up table variable structure control (TVSC) needs less time to reach sliding surface and less tracking error. Larger β value needs larger torque at initial time, and less tracking time is observed. We also found the proposed TVSC needs β large enough to overcome the uncertainties and the bounded noise. In case the β value is not enough large, it does not guarantee the tracking error is zero eventually. In this paper, we suppose that a huge torque can be supplied in actual manipulator application, and the simulation is an ideal circumstance. But in actual condition, maybe the torque can not be supplied so large. It results that the tracking trajectory needs more time to track the designed target. Further, as soon as sliding variable reaches to zero, the tracking error trajectory will decay to zero at exponential rate. By properly adjusting the constants c_1 and c_2, the decaying velocity will be altered. Additional simulation, which is not shown here, shows that the proposed variable structure control with look-up table control law can deal with external disturbance very well.

4 Conclusion

A variable structure control with look-up table is proposed in this paper. The strategy involves calculating off-line the amount of future control that the two-link robot arm will need according to different angle position. Then a suitable control torque is picked up from the established table automatically and rapidly. The controller retains the benefits of variable structure control, i.e., insensitivity against parametric uncertainties and external disturbances. The significant advantages are that computing time has been saved and expensive prime cost is not necessary. Further we do not need to measure and observe the joint angle velocities.

References

[1] Itkis U, Control systems of variable structure. John Wiley & Sons, New York, 1976.

[2] Utkin VI, Variable structure systems with sliding mode. IEEE Trans Automa Contr 22:212-222, 1977.

[3] Utkin VI, Application of equivalent control method to the systems with large feedback gain. IEEE Trans Automa Contr 23:484-486, 1978.

[4] Hung JY, Gao W, Hung JC, Variable structure control: a survey. IEEE Trans Ind Electron 40:2-22, 1993.

[5] Stadler W, Analytical Robotics and Mechatronics. McGRAW-HILL, NewYork, 1995.

[6] Hsu L, Costa RR, Lizarralde F, Da Cunha JPVS, Dynamic positioning of remotely operated underwater vehicles. IEEE Robot Automa Mag 7:21-31, 2000.

[7] Kavoussanos M, Pouliezos A, Visionary automation of sack handling and emptying. IEEE Robot Automa Mag 7:44-49, 2000.

[8] Suzuki Y, Tsuchiya S, Okuyama T, Takahashi T, Nagai Y, Kimura S, Mechanism for assembling antenna in space. IEEE Trans Aerosp Electron Syst 37:254-265, 2001.

[9] Kiguchi K, Fukuda T, Robot manipulator contact force control application of fuzzy-neural network. Robotics and Automation , 1995 IEEE International Conference , vol. 1, pp. 875-880, May 1995.

[10] Ming Liu, Decentralized control of robot manipulators: nonlinear and adaptive approaches. Automatic Control, IEEE Transactions, vol. 44, pp. 357-363, 1999.

[11] F.Y. Hsu, L.C. Fu, Nonlinear control of robot manipulators using adaptive fuzzy sliding mode control. Intelligent Robots and Systems 95, 1995 IEEE/RSJ International Conference, vol. 1, pp. 156-161, Aug. 1995.

[12] Ham C, Qu Z, Johnson R, Robust fuzzy control for robot manipulators**.** Control Theory and Applications, IEE Proceedings, vol. 147, pp. 212-216, 2000.

Appendix

$$A_{33} = \frac{0.49\sin(x_2)x_4 + (0.68+0.36\cos(x_2))(0.36\sin(x_2)x_3)}{1.41+0.49\cos(x_2)-(0.68+0.36\cos(x_2))^2}$$

$$A_{34} = \frac{0.24\sin(x_2)x_4}{1.41+0.49\cos(x_2)-(0.68+0.36\cos(x_2))^2}$$

$$A_{43} = \frac{(-0.68-0.36\cos(x_2))(0.72\sin(x_2)x_4) + (2.08+0.72\cos(x_2))(-0.36\sin(x_2)x_3)}{1.41+0.49\cos(x_2)-(0.68+0.36\cos(x_2))^2}$$

$$A_{44} = \frac{(-0.68-0.36\cos(x_2))(0.36\sin(x_2)x_4)}{1.41+0.49\cos(x_2)-(0.68+0.36\cos(x_2))^2}$$

$$B_{31} = \frac{0.68}{1.41+0.49\cos(x_2)-(0.68+0.36\cos(x_2))^2}$$

$$B_{32} = \frac{-0.68-0.36\cos(x_2)}{1.41+0.49\cos(x_2)-(0.68+0.36\cos(x_2))^2}$$

$$B_{41} = \frac{-0.68-0.36\cos(x_2)}{1.41+0.49\cos(x_2)-(0.68+0.36\cos(x_2))^2}$$

$$B_{42} = \frac{2.08+0.72\cos(x_2)}{1.41+0.49\cos(x_2)-(0.68+0.36\cos(x_2))^2}$$

$$G_3 = \frac{-12\cos(x_1)+2.12\cos(x_2)\cos(x_1+x_2)}{1.41+0.49\cos(x_2)-(0.68+0.36\cos(x_2))^2}$$

$$G_4 = \frac{12\cos(x_1)+6.35\cos(x_1)\cos(x_2)-\cos(x_1+x_2)(8.23+2.12\cos(x_2))}{1.41+0.49\cos(x_2)-(0.68+0.36\cos(x_2))^2}$$

Table 1. Look-up table 1: $\tilde{\tau}_1$ and $\tilde{\tau}_2$

q_2 \ q_1	-180°		-170°		$\cdots$	180°	
-180°	$\tilde{\tau}_1$	$\tilde{\tau}_2$	$\tilde{\tau}_1$	$\tilde{\tau}_2$	$\cdots$	$\tilde{\tau}_1$	$\tilde{\tau}_2$
	-21.81	0.67	-21.53	0.39	$\cdots$	-21.81	0.67
-170°	$\tilde{\tau}_1$	$\tilde{\tau}_2$	$\tilde{\tau}_1$	$\tilde{\tau}_2$	$\cdots$	$\tilde{\tau}_1$	$\tilde{\tau}_2$
	-21.63	0.58	-21.53	0.12	$\cdots$	-21.63	0.58
$\vdots$	$\vdots$	$\vdots$	$\vdots$	$\vdots$	$\ddots$	$\vdots$	$\vdots$
180°	$\tilde{\tau}_1$	$\tilde{\tau}_2$	$\tilde{\tau}_1$	$\tilde{\tau}_2$	$\cdots$	$\tilde{\tau}_1$	$\tilde{\tau}_2$
	-21.81	0.67	-21.53	0.39	$\cdots$	-21.81	0.67

Table 2. Look-up table 2: $\hat{\mu}$

q_2 \ q_1	-180°		-170°		$\cdots$	180°	
-180°	1.36	0.32	1.37	0.33	$\cdots$	1.36	0.32
	0.32	0.68	0.33	0.68	$\cdots$	0.32	0.68
-170°	1.36	0.32	1.37	0.33	$\cdots$	1.36	0.32
	0.32	0.68	0.33	0.68	$\cdots$	0.32	0.68
$\vdots$	$\vdots$	$\vdots$	$\vdots$	$\vdots$	$\ddots$	$\vdots$	$\vdots$
180°	1.36	0.32	1.37	0.33	$\cdots$	1.36	0.32
	0.32	0.68	0.33	0.68	$\cdots$	0.32	0.68